Seasonal Variations of Water Mass Distributions and Their Causes in the Yellow Sea, the East China Sea and the Adjacent Seas of Cheju Island

Ig-Chan PANG · Hong-Kil RHO and Tae-Hee KIM

Department of Oceanography, Cheju National University,
Cheju 690-120, Korea

Seasonal variations of water mass distributions in the Yellow Sea, the East China Sea, and the adjecent seas of Cehju Island, are investigated. A common seasonal variation over these whole areas is shown. Warm and saline waters are extended northwestward into the Yellow Sea in winter and retreated back southeastward to the East China Sea in summer. Barotropic numerical model results suggest that monsoon winds could drive such seasonal variations. Upwind flows play an important role in the processes. In the numerical model results, upwind flows are shifted to China. It is due to energy dissipations by complicated coast lines and shallow bottom topographies in the northern part of the Yellow Sea. The shifted routes of upwind flows agrees well with that of the southward extensions of the Yellow Sea Bottom Cold Waters in summer.

Introduction

There are significant water mass movements in the Yellow Sea, the East China Sea, and the adjacent seas of Cheju Island, such as the southward extensions of Yellow Sea Bottom Cold Waters (Asaoka & Moriyasu, 1966; Nakao, 1977; Lie, 1984; Park, 1985, 1986; Kim et al., 1991; Yoon et al., 1991), the northeast movements of Yangzee Diluted Waters to the Cheju Strait(Yu et al., 1983; Beardsley et al., 1983; Zhao et al., 1983), and Yellow Sea Warm Current(Uda, 1934; Byun & Chang, 1988; et al.). Such seasonal water mass movements seem to cause seasonal variations of water mass distributions. Specially, the seasonal variations seem to be related to the argument of Yellow Sea Warm Current. Since Uda's suggestion(1934), there have been negative opinions(Lie, 1984, 1985; Nakao, 1977; Kim et al., 1991; et al.) as well as positive opinions (Byun and Chang, 1988; et al.) of its existence. The arguments of Yellow Sea Warm Current possi-

bly arise from different seasons of observation. Therefore, seasonal variations are important to understand the water mass movements in these areas. In this paper, the seasonal variations of water mass distributions and the related water mass movements are investigated as follows:

First, the seasonal variations of water mass distribution in the Yellow Sea, the adjacent seas of Cheju Island, and the East China Sea are investigated. It is shown that there is a common seasonal variation over the whole areas.

Next, the related water mass movements are investigated numerically. They have been simulated in a barotropic model. As forcing, monsoon winds and variations of Kuroshio transports are used. It is shown that the monsoon winds could drive the seasonal circulations.

Finally, the shift of upwind flows, shown in the numerical model results, is interpreted by using the wave model of coastally trapped waves.

The purpose of this study is to understand the

seasonal circulations in these areas through the seasonal variations of water mass distributions.

Seasonal Variations of Water Mass Distributions

To see the seasonal variations of the distributions of warm and saline waters in the Yellow Sea, the far-west section shown in Fig. 1, linking the station 10's of 307−314 lines of the National Fisheries Research and Development Agency of Korea, is chosen. Fig. 2 is the time variations of temperature and salinity on the depth of 50m along the section. Dotted areas in Fig. 2 show the distributions of warm and saline water above 10℃ and 33.0 ‰. Those are by and large the upper limits of Yellow Sea Bottom Cold Waters(Nakao, 1977; Lie, 1984; Inoue, 1974; Kondo, 1985; Youn et al., 1991).

In Fig. 2, the warm and saline waters are extended northward up to the middle of Yellow Sea in winter and retreated back in summer. These sea-

Fig. 1. Bottom topographies in the Yellow and the East China Seas and the Section along the station 10's in 307~314 hydrographic lines of the National Fisheries Research and Development Agency of Korea.

sonal variations indicate northward intrusions of Yellow Sea Warm Waters in winter and southward extensions of Yellow Sea Bottom Cold Waters in summer. However, there is a different opinion that the distributions of water characteristics in the Yellow Sea could be formed mostly by the effects of eddy diffusions without advections(Lee and Kim, 1989). Although, the seasonal variations shown in Fig. 2 are hard to be explained only by diffusions, they should be explained by the connections of the seasonal variations in the adjacent seas of Cehju Island and the East China Sea.

Fig. 3 shows the bimonthly variations of water mass distributions below the depth of 50m in the adjacent seas of Cheju Island(Rho, 1985). It is obtained by water mass analyses with the 10(1970~1979) years data of the National Fisheries Research and Development Agency of Korea. All data in the areas are plotted in T-S diagram in each month and each year. Then two extreme water characteristics are shown: the warmest & most saline and the coldest & least saline. The water masses (except coastal waters) are identified as mixtures of two extremes. The water masses are classified into 6 groups by mixing rate and distribution area: Tsushima Water, Yellow Sea Warm Water, Mixing Water(between Tsushima Water and Yellow Sea Cold Water), Yellow Sea Cold Water, Yellow Sea Bottom Cold Water and Coastal Water. The mixing rates used here are shown in Table 1. Coastal Water is distinguished from other waters. This classification of water masses by mixing rates is to solve difficulties from the variations of water characteristic values by month and year. Fig. 3 shows the water mass distributions appeared most frequently in 10 years. Fig. 3 shows that in the adjacent seas of Cheju Island warm and saline waters are also extended northwestward to the Yellow Sea in winter and retreated back southeastward in summer. (The seasonal variations of cold and less saline water are not so clear, partly due to the staticstical processes.)

The same tendency of seasonal variations in the Yellow Sea and the adjacent seas of Cheju Island could be found in the East China Sea. Fig. 4 shows salinity distributions at 50m depth in winter and
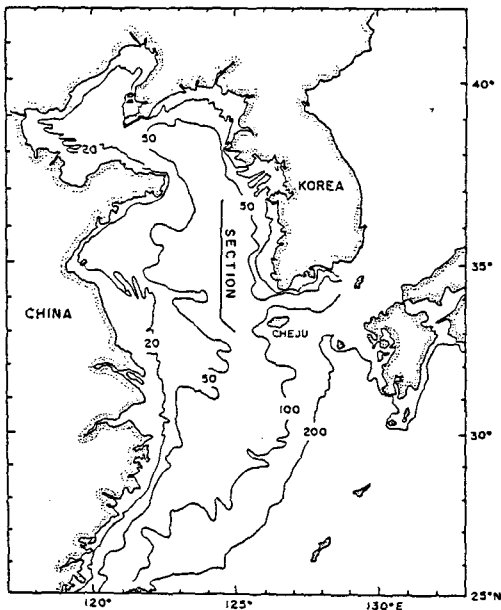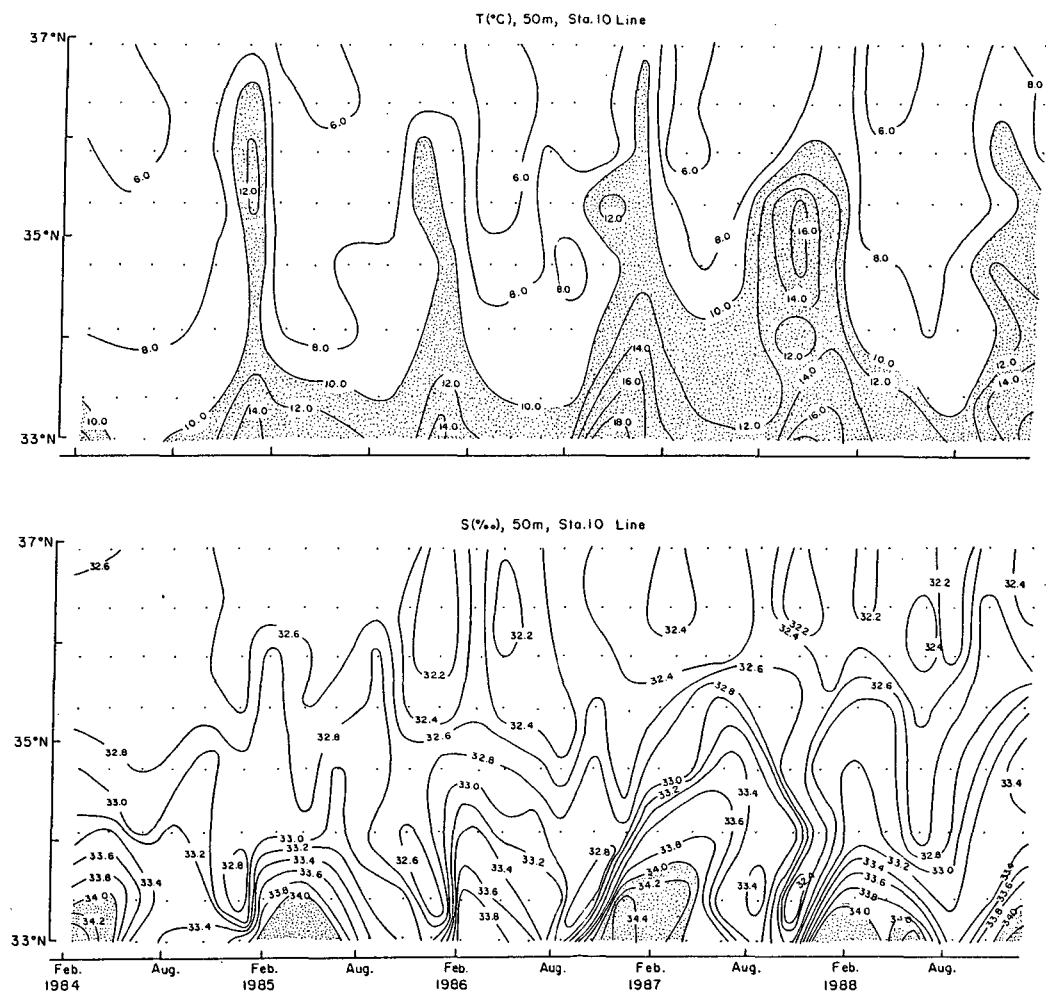
Fig. 2. Variations of temperature and salinity distributions on the layer of 50m depth along the station 10's in 307~314 hydrographic lines of the National Fisheries Research and Development Agency of Korea, in 5 years.

Table 1. Mixing rates of two extremes in each water mass. One is the warmest and most saline and the other is the coldest and least saline. Two extremes are obtained from T-S diagram for each month and each year.

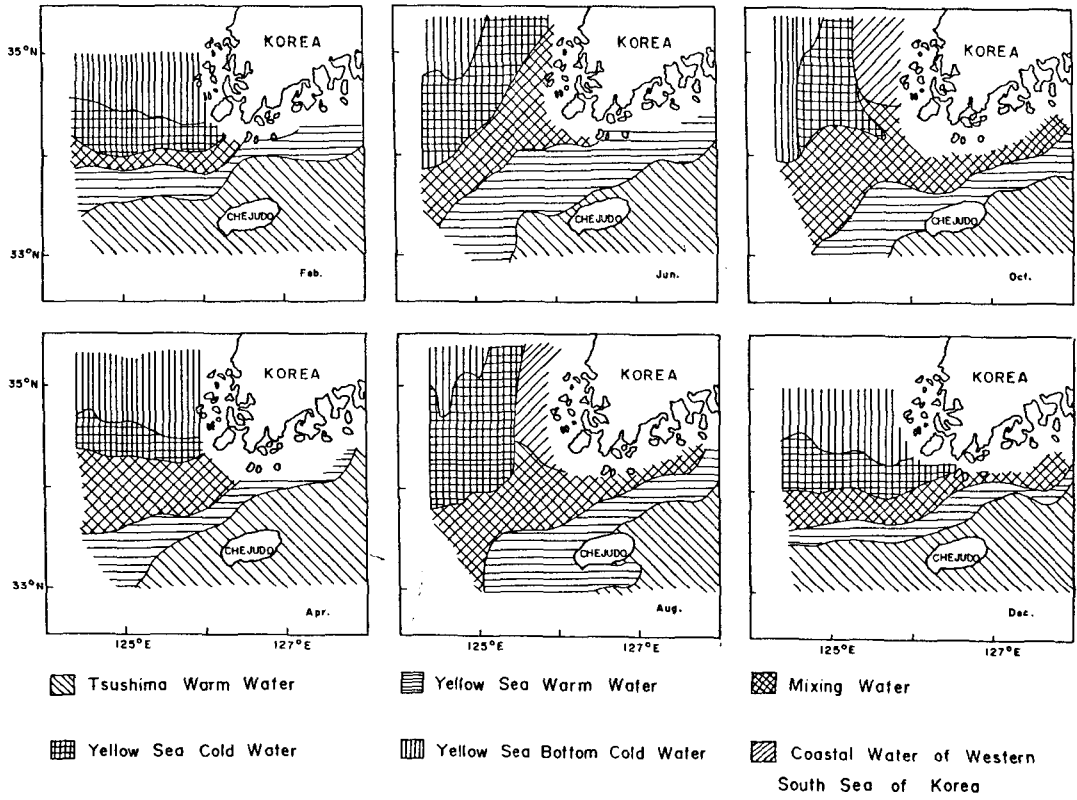|	Tsushima water	Yelow Sea warm water	Mixing water	Yellow Sea cold water	Yellow Sea Bottom cold water
warmest and most saline extreme	100~75%	75~60%	60~40%	40~25%	25~ 0%
coldest and least saline extreme	0~25%	25~40%	40~60%	60~75%	75~100%

Fig. 3. Bimonthly variations of water mass distributions around Cheju Island (from Rho, 1985).
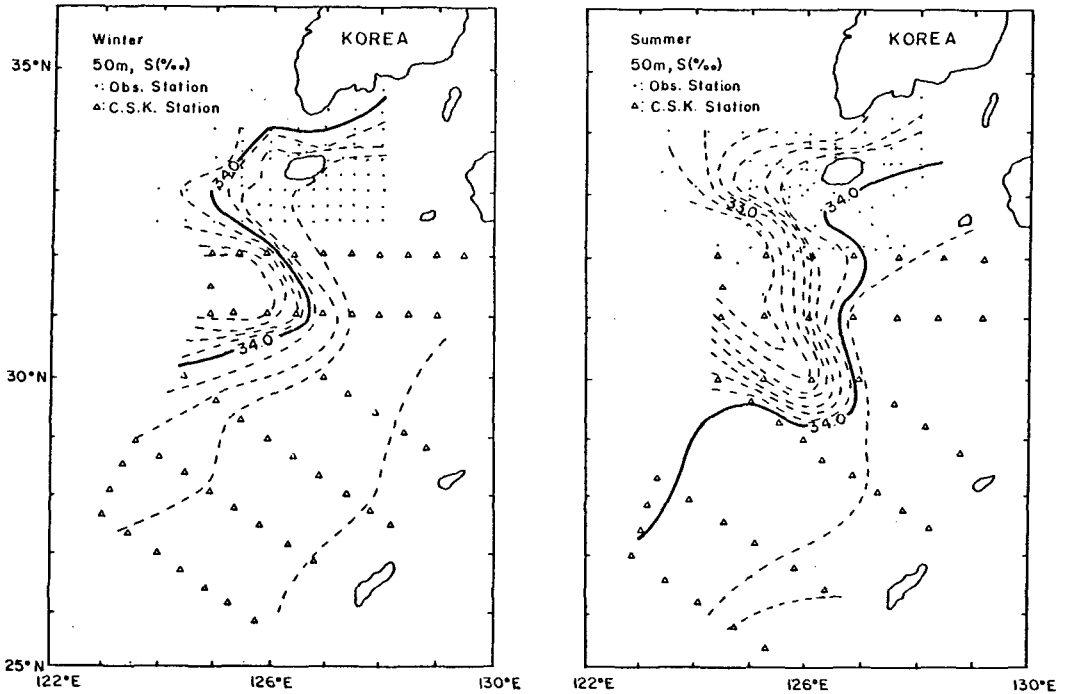

Fig. 4. Salinity distributions on the layer of 50m depth in the East China Sea (a) in winter and (b) in summer.

summer, by combining CSK data and data obtained from Cheju National University. The southward extension of less saline(and cold) waters in summer is clearly shown. Compared to the bottom topography in Fig. 1, the core axis of less saline water nearly coincides with the isobath line of 50m, as reported by Kim et al.(1991) and Youn et al. (1991). On the other hand, the saline waters are extended northwestward to the Yellow Sea in winter and retreated back southeastward in summer.

The common seasonal variation of water mass distributions over the Yellow Sea, the East China Sea, and the adjacent seas of Cheju Island seems to be characterized as the northward intrusions of Yellow Sea Warm Water in winter and the southward extensions of Yellow Sea Bottom Cold Water in summer.

Simulated Seasonal Circulations

In this section, the circulation to drive the seasonal variations shown in the preceeding section is simulated by a barotropic numerical model. A numerical finite-difference method has been used. The equations of vertically averaged motion and continuity are, as usual,

$$\frac{\partial u}{\partial t} + u\frac{\partial u}{\partial x} + v\frac{\partial u}{\partial y} - fv + \frac{ku(u^2+v^2)^{1/2}}{H} + g\frac{\partial \zeta}{\partial x}$$

$$-A_H(\frac{\partial^2 u}{\partial x^2} + \frac{\partial^2 u}{\partial y^2}) - \frac{\rho_a C_d W_x}{\rho H} = 0 \qquad (1)$$

$$\frac{\partial v}{\partial t} + u\frac{\partial v}{\partial x} + v\frac{\partial v}{\partial y} + fu + \frac{kv(u^2+v^2)^{1/2}}{H} + g\frac{\partial \zeta}{\partial y}$$

$$-A_H(\frac{\partial^2 v}{\partial x^2} + \frac{\partial^2 v}{\partial y^2}) - \frac{\rho_a C_d W_y}{\rho H} = 0 \qquad (2)$$

$$\frac{\partial \zeta}{\partial t} + \frac{\partial}{\partial x}(Hu) + \frac{\partial}{\partial y}(Hv) = 0 \qquad (3)$$

where x, y: Cartesian coordinate, positive eastward, northward, respectively

u, v: respective components of depth mean current in the directions of x, y

t: time

f: Coriolis parameter

ζ: elevation of sea surface

H: total depth of water

k: coefficient of bottom friction

A_H: horizontal eddy diffusion coefficient.

ρ, ρ_a: densities of water and air, respectively

C_d: drag coefficient

W_x, W_y: respect components of wind speeds in the directions of x, y.

The vertically averaged currents and advective terms are defined as usual. These equations are applied to the Yellow Sea and East China Seas. Fig. 5 shows the study areas and bottom topography. β plane is applied and the coefficients of bottom friction(k), drag(C_d), and horizontal eddy diffusion (A_H) are 0.0002, 1.4×10^{-3}, and $10^4(m^2/sec)$, respectively. Basic currents are driven by Kuroshio transports and seasonal circulations are driven monsoon winds. The monsoon winds are simplified as a northerly wind in winter and a southerly wind in summer. The winds are steady and of 10m/sec. The Kuroshio current flows in from the southern open boundary and out through two eastern open boundaries: the Korea Strait and the southern sea of Japan. The inflow is evenly distributed along the southern boundary, and its total transport is 30 Sv. A free radiation boundary condition is applied to
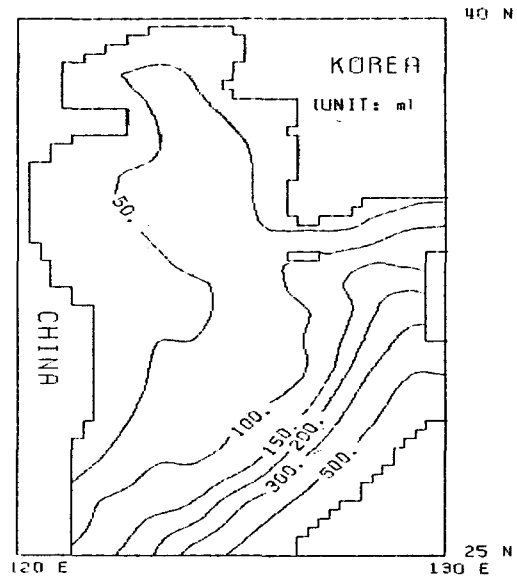

Fig. 5. Model areas and bottom topographies used in the numerical model.

the wastern boundaries(Rφed and Cooper, 1985), as follows:

$$\frac{\partial Q}{\partial t} + C\frac{\partial Q}{\partial n} = 0 \qquad (4)$$

where Q, C and n are any of model dependent variables, the propagation speed, and coordinate normal to the open boundary, respectively. Figs. 6, 7 and 8 are the results driven by only Kuroshio transport, Kuroshio transport and northerly wind, and Kuroshio transport and southerly wind, respectively. They show steady state currents. In the figures, the figures (A) are the same as the figures (B), but have a different scale of arrow magnitude, to see clearly the flows in the Yellow Sea.

The basic currents driven by Kuroshio transport are strong in the East China Sea, but only negligible in the Yellow Sea(in Fig. 6). The flows in the Yellow Sea are very small($0\{<0.5cm/sec\}$) compared to the Kuroshio flows($0\{1knot\}$). Variations of Kuroshio transport change flow magnitudes, but not flow patterns.

However, winds drive significant flows in the Yellow Sea. Fig. 7 and 8 show the flows of $0(5cm$/sec) in the Yellow Sea driven by the monsoon wi-

nds of $10m$/sec over the basic flow shown in Fig. 6. In the southern part of the Yellow Sea, upwind flows in the middle of the Yellow Sea and downwind flows along coasts are shown well. Such flows are changed reversely with seasons by monsoon winds. In the northern part of the Yellow Sea, the flow patterns are complicated due to the coastline. Upwind and downwind flows form local eddies. Nevertheless, the flow directions are basically upwind in the middle and downwind along the coasts.

In the southern part of the Yellow Sea, the directions of upwind flow driven by monsoon winds are rather northwestward into the Yellow Sea in winter and southeastward out of the Yellow Sea in summer. This is well consistent with the seasonal variations shown in the preceeding section.

It is to be noted that the axes of upwind flow do not coincide with the deep trough of the Yellow Sea. They are shifted to China coast, which agree with the route of southward extensions of Yellow Sea Bottom Cold Waters in summer shown in the preceeding section and some previous reports(Xie et al., 1983; Kim et al., 1991; Youn et al., 1991). The axis shift may be a part reason Yellow Sea Warm Current has been hard to be detected with
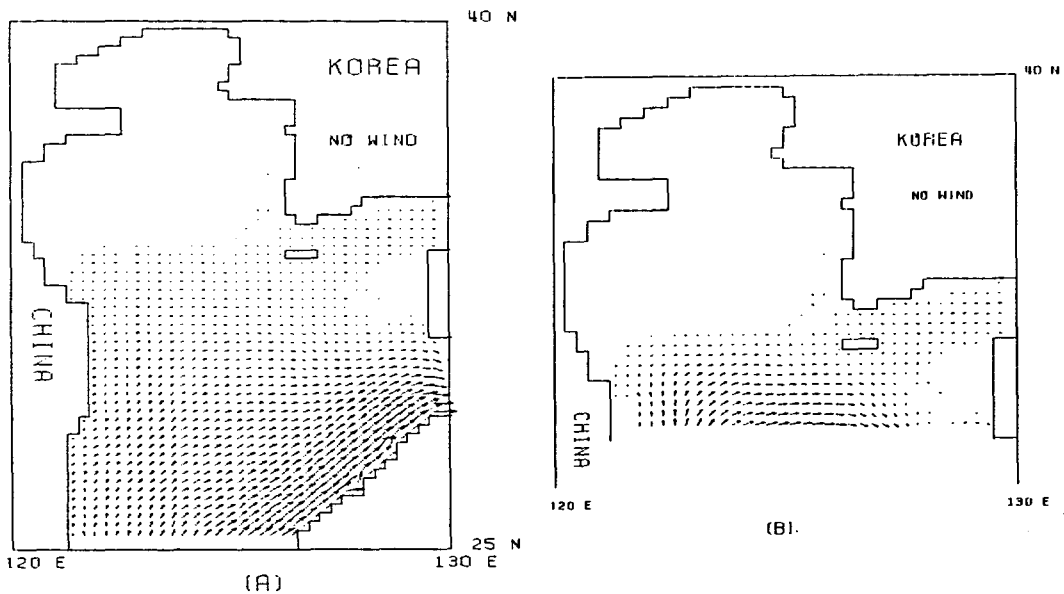

Fig. 6. Numerical result of the circulations driven by only Kuroshio transport. A is the same results as B, with a different scale of velocity magnitude.
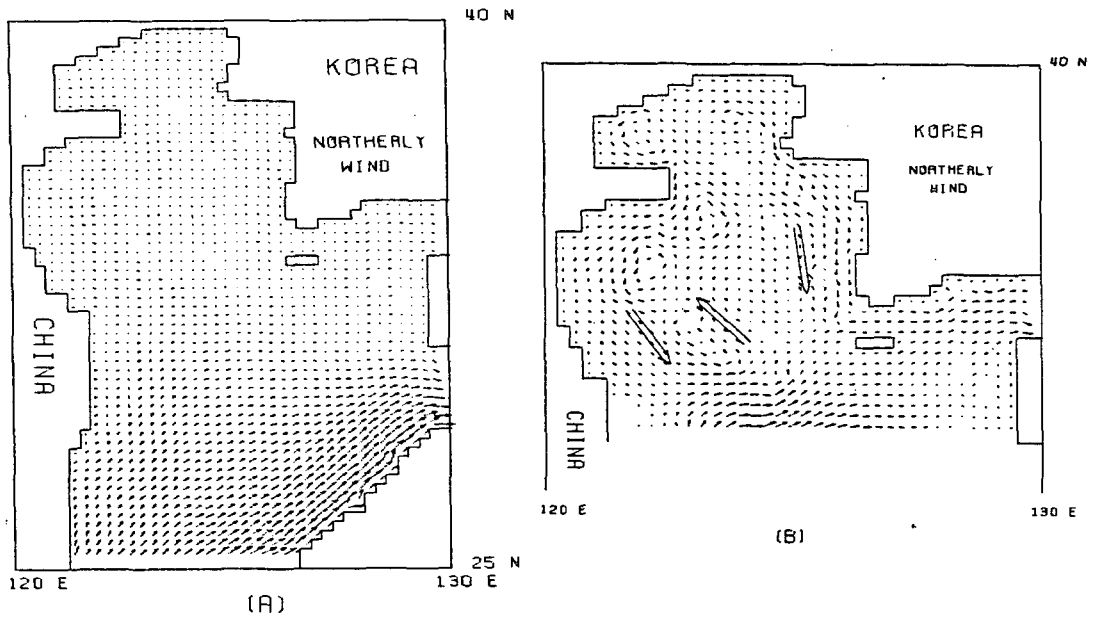
Fig. 7. Numerical result of the circulations driven by the Kuroshio transport and northerly winds. A is the same results as B, with different scale of velocity magnitude.
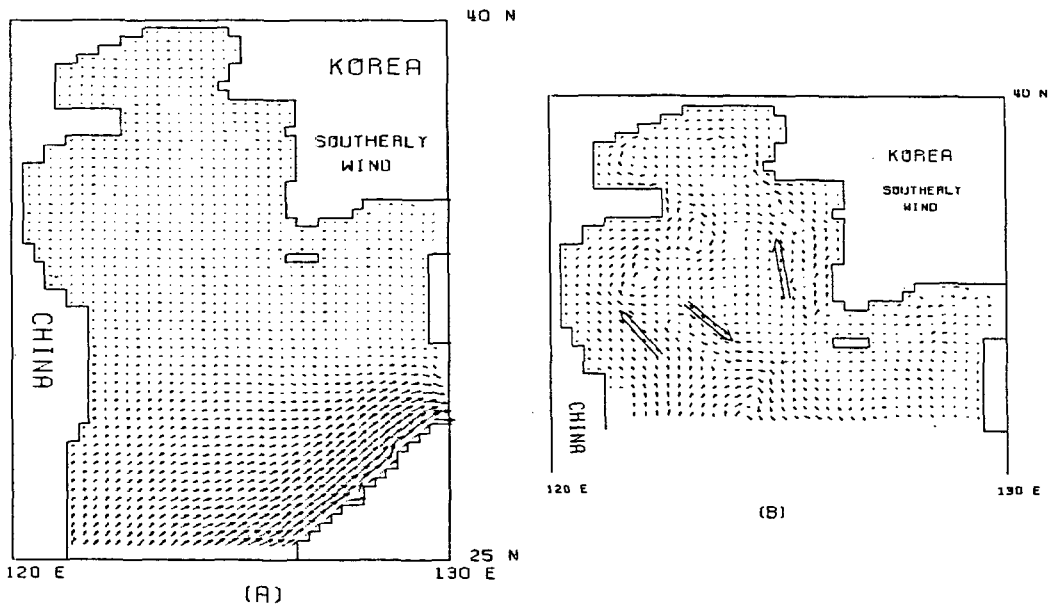

Fig. 8. Numerical result of the circulations driven by the Kuroshio transport and southerly winds. A is the same results as B, with different scale of velocity magnitude.

most hydrographic data near Korean coast. In the next section, the axis shifts are interpreted by the wave model of coastally trapped waves.

Axis shift of upwind flows

The theory of upwind flows has been qualitatively applied to the Yellow Sea(Park, 1986), and observed upwind flow events have been reproduced by the wave model of coastally trapped waves (Pang, 1987; Hsueh and Pang, 1989). However, the shift of upwind flows to China is not predicted by them, because it is hard to estimate, by a simple theory or a analytical wave model, how much energy is dissipated due to the complicated coastlines in the northern part of the Yellow Sea.

In the Yellow Sea, there are two sets of coastally trapped waves propagating oppositely(Pang, 1987; Hsueh and Pang, 1989). One set is propagating northward and the other is propagating southward. Because the northern part of Yellow Sea is closed, the northward waves return back. In these processes, they lose their energy due to complex coast lines and shallow water depths. The combinations of northward waves and dissipated southward waves determine the velocity fields as well as sea surface fields. Wave functions are calculated by the integration of the following wave equation along the characteristics.

$$-\frac{1}{C_n}\frac{d\phi_n}{dt} + \frac{d\phi_n}{dy} + \sum_{m=-\infty}^{\infty} a_{mn}\phi_m = (b_{1n} - b_{2n})T^y \quad (5)$$

where $n = -\infty \cdots, -3, -2, -1, 1, 2, 3, \cdots \infty$(two sets)

$$a_{mn} = \frac{1}{f \cdot s_n} \left[-rF_{mx}F_n \Big|_{-B1}^{B2} + \int_{-B1}^{B2} \frac{drF_{mx}}{dx} F_n dx \right]$$

$$b_{1n} = F_n(-B1)/r_n$$

$$b_{2n} = F_n(B2)/r_n$$

$$s_n = -HF_n^2 \Big|_{-B1}^{B2} + \int_{-B1}^{B2} \frac{dH}{dx} F_n^2 dx$$

and x, y: Cartesian coordinates in the directions of cross-shelf and along the shelf

H: water depth

ϕ_n: nth mode wave function in the normal mode expression of pressure, p(x, y, t) $= \Sigma F_n(x)\phi_n(y, t)$

F_n: nth mode of eigenfunctions

C_n: phase speed of nth mode

r_n: friction coefficient of nth mode

T^y: y-component of wind stress

$-B1$: x-coordinate of China coastal boundary

$B2$: x-coordinate of Korea coastal boundary.

The schmatic coordinate system is shown in Fig. 9. x and y coorinates refer to the cross-shelf(positive eastward) and the alongshore(positive northward) directions, respectively. B1 and B2 are the coastal boundary locations and H_O is the deepest water depth. The values of B1, B2 and H_O chosen here are 400km, 80km, and 100m, respectively.
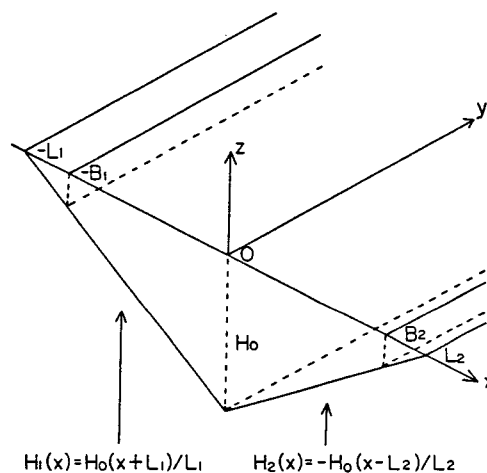

Fig. 9. Schematic channel cross section of the Yellow Sea and coordinates incorporated in the wave model of coastally trapped waves. x and y coordinates refer to the the cross-shelf (positive eastward) and the alongshore (positive northward) directions, respectively.

For a barotropic case, the 1st modes of continental shelf waves contribute the most to velocity fields(Pang, 1987; Hsueh and Pang, 1989). The axis shift of upwind flows can be qualitatively investigated with the 1st modes calculated from the equation (5). In Figs. 10, the combined sea surface elevations of them in the cross-shelf direction are shown for four different friction coefficients, 0, 10^{-4}, 10^{-3} and 10^{-2}, respectively. Y-axis represents a non-dimensional amplitude of sea surface elevations. Northly winds of 10m/sec are applied.
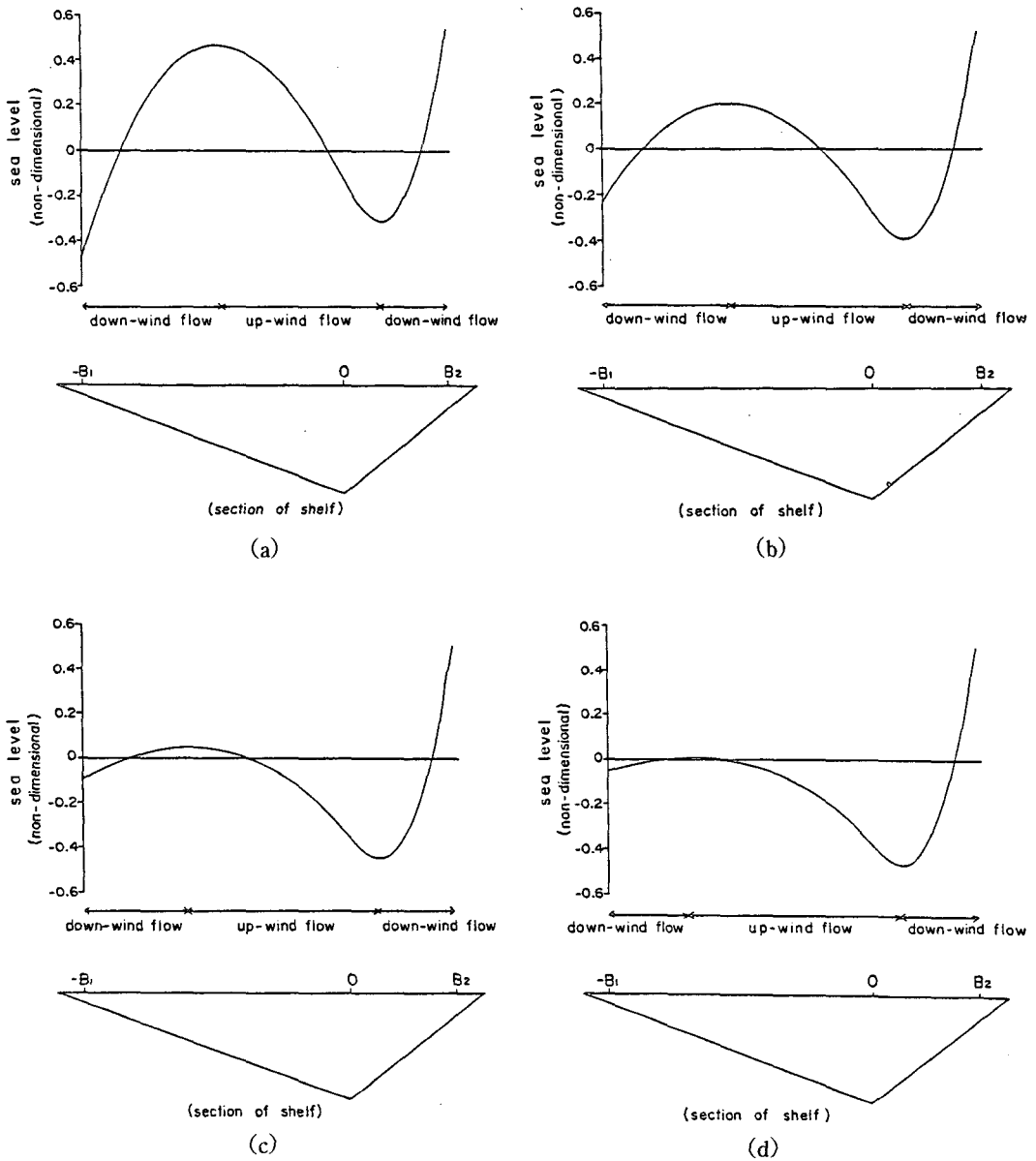
Fig. 10. Sea surface elevations across the shelf obtained by the wave model (a) with frictional coefficient of 0 (no energy dissipation), (b) with frictional coefficient of 10^{-4}, (c) with frictional coefficient of 10^{-3}, and (d) with frictional coefficient of 10^{-2}.

For a large-scale and low-frequency flow of coastally trapped waves, momentum balances in cross-shelf (x) directions are geostrophic. Therefore, sea surface elevations in the cross-shelf direction show alongshore currents. Negative gradients of sea level in x-direction imply southward(out of the paper) alongshore flows which are upwind flows for nor- thly winds applied in this case, and vice versa. Fig. 10 shows that the ranges of upwind flows are shifted to China coast with increases of energy dissipations. (At the same time, downwind flows along China coast become weaker.) It means that energy dissipations by complex coast lines and shallow water depths in the northern part of the Yellow

Sea cause up-wind flows to be shifted to China.

Results

A common seasonal variation of water mass distributions is shown in the East China Sea, the Yellow Sea, and the adjacent seas of Cheju Island (Figs. 2, 3, 4). Warm and saline waters(Tsushima waters or Yellow Sea Warm Waters) are extended northwestward into the Yellow Sea in winter and retreated back southeastward to the East China Sea in summer. The seasonal variations seem to be caused by seasonal circulations such as the northward intrusions of Yellow Sea Warm Water in winter and the southward extension of Yellow Sea Bottom Cold Water in summer.

Such seasonal circulation has been simulated. The monsoon winds drive significant seasonal flows in the Yellow Sea: northwestward into the Yellow Sea in winter and southeastward to the East China Sea in summer. The seasonal flows are consistent the seasonal variations of water mass distributions.

The upwind flows shown in the numerical model results do not follow the deep trough of the Yellow Sea(compare Figs. 7, 8 with Fig. 1), but are shifted to China coast. The wave model results of coastally trapped waves show that shifts of upwind flows are due to the energy dissipations by complex coast lines and shallow water depths in the northern part of the Yellow Sea. The upwind flows along the isobath of $50m$ in the numerical model results agree with the route of southward extensions of Yellow Sea Bottom Cold Waters in summer shown in Fig. 3 and some previous reports(Xie et al., 1983; Kim et al., 1991; Youn et al., 1991).

Discussions

We have some limitations in this study. One is the deduction of circulations from the water
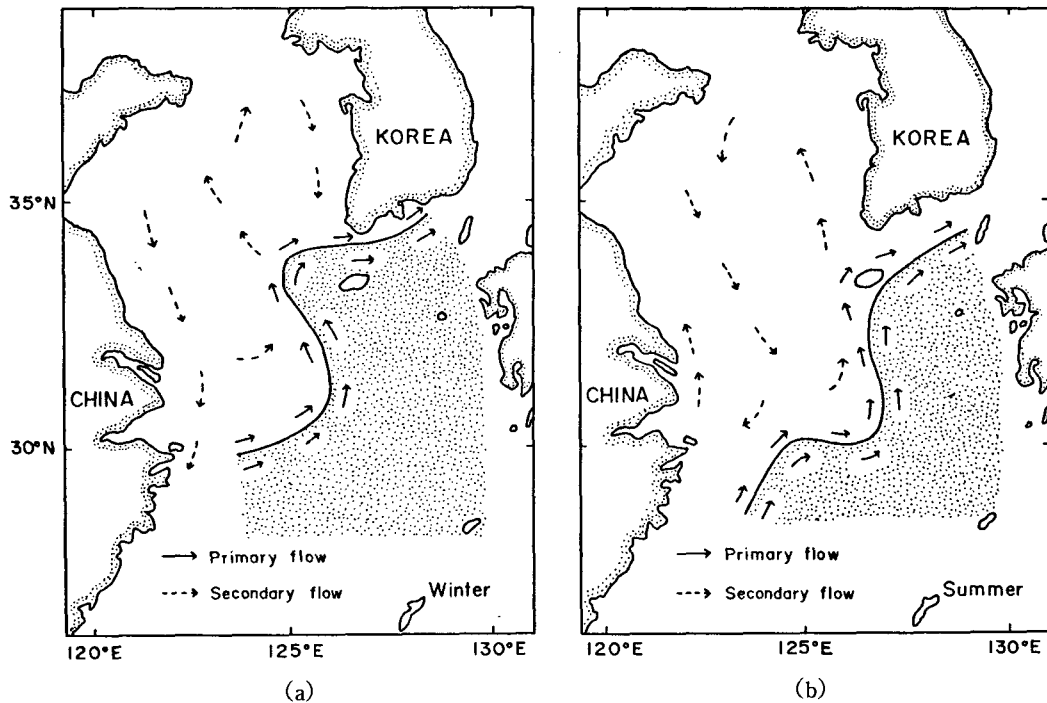

Fig. 11. A schematic circulation diagram in the Yellow Sea and the East China Sea (a) in winter and (b) in summer, based on the two circulations: primary one driven by Kuroshio transport and secondary one driven by monsoon winds.

mass distributions. However, the deduction is based on the assumption that the circulation should be the major factor to cause such large scale variations. Another is a possibility of baroclinic flows, specially in summer. Only the barotrophic part is investigated in this study. However, they might not be so significant compared to barotrophic flow. A theoretical criterion of baroclinic flow due to stratification over a sloping bottom is given as Ns/f > 1 by Clarke and Brink(1985), where N, s and f are Brunt Väsälä frequency, bottom slope, and Coriolis parameter. Typical values of them in the Yellow Sea in summer could be respcetively 2×10^{-2}, 10^{-3}, 8.5×10^{-5} so that Ns/f≒1/4<1. It suggests that barotrophic responses of stratified oceans tend to be major parts in this area.

In spite of some limitations, the numerical model results show a possibility of two kinds of circulations in the Yellow Sea and the East China Sea. One is driven by Kuroshio Current and the other is driven by monsoon winds. While the former(primary circulation) is strong and persistent through the year, the latter(secondary circulation) is weak and reversible with seasons. The primary flows can be represented by Tsushima Current. Fig. 11 shows a schematic circulation diagram based on the two circulations. Dots show Tsushima Water areas, which are chosen by the isohaline of 34 ‰ in Fig. 4. The solid arrows do not represent the major Tsushima Current. They show only primary flows along the boundaries of Tushima Waters. The whole primary flows are not drawn in details. Most waters west of Cheju Island flow out eastward through the Cheju Strait, as reported(Kim et al., 19 81). The water mass movements into the Yellow Sea by the secondary circulation might not be in the forms of branching current, as presented by Uda(1934).

Another seasonal flows related to such circulations is the movements of Yangtze diluted waters in summer. In summer, Yangtze coastal waters flow over to the Cheju Strait(Kim, 1986). It seems to be understandable if they follow the summer seasonal circulation shown in Fig. 11. A imaginable route would be to flow northward and offshore first off Yanzgtze river, thereafter, turn to the south by

southward upwind flows, turn to the north again by northward primary flows and then eventually get to the Cheju Strait.

References

Asaoka, O. and S. Moriyasu. 1966. On the circulation in the East China Sea and the Yellow Sea in winter(Preliminary Report). Oceanogr. Mag., 18(1−2): 73~81.

Beardsley, R. C. and R. Limeburner. 1983. Structure of the Changjiang River Plume in the East Chnia Sea during June 1980: Sedimentation on the Continental Shelf with Special Reference to the East China Sea. Acta, editor, Oceanologica. Sinica. China Ocean Press, Beijing, 243~260.

Byun, S. K. and K. I. Chang. 1988. Tsushima Current Water at entrance of the Korea Strait in Autumn. Prog. Oceanog., 21: 295~296.

Clarke, A. J. and K. H. Brink. 1985. The response of stratified, frictional flow of shelf and slope waters to fluctuating large-scale, low-frequency wind forcing. J. Phys. Oceanogr., 15: 439~453.

Hsueh, Y. and I. C. Pang. 1989. Coastally Trapped Long Waves in the Yellow Sea. J. Phys. Oceanogr., 19(5): 612~625.

Inoue, N. 1974. Oceanography Characterisitcs in the western sea of Japan. in: Tsushima Warm Current, edited by Japan Fishery Society, Fishery Science series: 27~41.

Kim, I. O. 1986. A study on coastal waters of the China Continent appeared in the neighbouring seas of Cheju Island. MS thesis, Cheju National Univ., 46p.

Kim, K., H. K. Rho and S. H. Lee. 1991. Water masses and circulation around Cheju-Do in summer. J. Oceanog. Soc., 26(3): 262~277.

Kondo, M. 1985. Oceanographic investigations of fishery grounds in the East China Sea I, Characteristics of the mean temperature and salinity distributions measured at 50m and near the bottom. Bull. Seikai Reg. Fish. Res. Lab., 62: 19~66.

Lee, G. T. and K. Kim. 1989. A study on the eddy

diffusion of salinity in the lower layer of the Yellow Sea. Yellow Sea Research, 2: 21~29.

Lie, H. J. 1984. A note on water masses and general circulation in the Yellow Sea(Hwanghae). J. Oceanog. Soc. Korea, 19: 187~194.

Lie, H. J. 1985. Wintertime temperature and salinity characteristics in the south-western Hwanghae(Yellow Sea). J. Oceanog. Soc. Japan, 41: 281~291.

Nakao, T. 1977. Oceanic variability in relation to fisheries in the East China Sea and the Yellow Sea. J. Fac. Mar. Sci. Technol., Tokai Univ. Spec. No. Nov., 199~366.

Nitani, H. 1972. Beginning of the Kuroshio: Kuroshio. Stommel, H. and K. Yoshida, editor, Univ. of Tokyo Press, Japan: 129~163.

Pang, I. C. 1987. Theory of Coastally Trapped Waves and its application to the Yellow Sea. Ph. D thesis, Florida State Univ., 128p.

Park, Y. H. 1985. Some important summer Oceanographic phenomena in the East China Sea. J. Oceanog. Soc. Korea, 21: 12~21.

Park, Y. H. 1986. A simple Theoretical Model for the Up-wind flow in the southern Yellow Sea. J. Oceanog. Soc. Korea, 21: 203~210.

Rho, H. K. 1985. Studies on marine environments of fishing grounds in the waters around Cheju Island, Ph. D. Thesis, Univ. of Tokyo: 215.

Røed, L. P. and C. K. Cooper. 1985. Open Boundary Conditions in Numerical Ocean Models. In Advanced Physical Oceanographic Numerical Modelling, edited by O'Brien J. J., D'Reidel Publishing Company, 411~436.

Uda, M. 1934. The results of simultaneous oceanographical investigations in the Japan Sea and its adjacent waters in May and June, 1932. J. Imp. Fisher. Exp. St., 5: 57~190.

Xie, Q., L. Zhang and F. Zhou. 1983. Features and Transportation of Suspended Matter over the continental shelf of the Changjiang Estuary: Sedimentation on the Continental Shelf with Special Reference to the East China Sea. Acta, editor, Oceanologica. Sinica. China Ocean Oress, Beijing, 370~381.

Youn, Yong-Hoon, Young-Hyang Park and Jong-Hon Bong. 1991. Enlightment of the Characteristics of the Yellow Sea Bottom Cold Water and its Southward Extension. J. Korean Earth Science Society, Vol. 12, No. 1, pp. 25~37.

Yu, H., D. Zheng and J. Jiang. 1983. Basic Hydrographic Characteristics of the Studied Area. Sedimentation on the Continental Shelf with Special Reference to the East China Sea. Acta, editor, Oceanologica. Sinica. China Ocean Oress, Beijing, 270~279.

Zhao, J., R. Qiao, R. Dong, J. Zhang and S. Yu. 1983. An analysis of of Current Conditions in the investigation area of the East China Sea: Sedimentation on the Continental Shelf with Special Reference to the East China Sea. Acta, editor, Oceanologica. Sinica. China Ocean Oress, Beijing, 288~301.

황해, 동지나해와 제주도 주변해역에서의
해수분포의 계절변화와 그 원인

방익찬 · 노홍길 · 김태회

제주대학교 해양학과

황해, 동지나해와 제주도 주변해역의 해수분포의 계절변화를 살펴본 결과 이 해역전반에 걸쳐 공통된 계절변화가 보였다. 고온고염의 해수는 겨울에 황해 쪽으로 확장되며 여름에 동지나해 쪽으로 후퇴한다. 순압모델결과는 계절풍이 이와 같은 해수분포의 계절변화를 유도할 수 있음을 보여준다. 역풍류는 이 과정에서 중요한 역할을 하는데, 모델결과에는 역풍류의 축이 중국 쪽으로 이동되어 나타난다. 역풍류 축의 이동은 황해북부의 복잡한 해안선과 얕은 해저지형에 의한 에너지손실에 기인한다. 수치모델결과에 나타난 이동된 역풍류의 길은 여름철 황해저층냉수 남하의 길과 잘 일치한다.